Convective transport of mass and energy in severe storms over the United States—an estimate from a geostationary altitude

By D. N. SIKDAR, V. E. SUOMI and C. E. ANDERSON, *The University of Wisconsin, Madison, Wisconsin, USA*

(Manuscript received November 4, 1969; revised version May 5, 1970)

ABSTRACT

Some important characteristics of intense convection associated with tornado vortices are described in a case study based on photographs of the United States on April 19 and 23, 1968, that were transmitted from NASA's geosynchronous satellite, ATS-3. The growth rates of a number of convection complexes as estimated from the satellite cloud photographs are studied. Based on a three-layer convection model, the upward fluxes of mass and energy in these severe storms are computed. The computed fluxes seem to be higher by at least one order of magnitude than in a moderate thunderstorm (Brown, 1967).

It is suggested that the pronounced growth rate of a convection complex as estimated on the ATS-3 satellite photographs should be an indication of the presence of severe storm cells below the cirrus canopy.

1. Introduction

The thunderstorm is of major importance in meteorology, not only because it is a weather hazard but also because it is an important link in the redistribution of energy from the lower to the upper troposphere.

For many years the study of severe thunderstorms has been inhibited by lack of data, partly because of the size and nature of the storms. Thunderstorm models and theories of cumulonimbus convection have been greatly influenced by the data gathered on small thunderstorms by the Thunderstorm Project (1959). The investigators tacitly assumed that the results of these small-scale studies could be extrapolated to explain more intense storms.

The Spin Scan Camera systems, University of Wisconsin experiments onboard ATS-1 and 3 geostationary satellites, have presented another aspect of the thunderstorm.

The purpose of this paper is to show that it is possible to isolate the regions of probable severe weather over the United States from the ATS-3 satellite cloud photographs and also to estimate the convective transport of mass and energy by deep convection in the mid-latitude disturbance field. This case study pertains to a satellite-observed cloud system over the United States on 19 and 23 April, 1968, when widespread tornado activity was reported by ground stations.

2. The severe local storm: A model

2.1 *Thermal stratifications in a severe storm*

In the past two decades a number of convection models have been proposed to explain the observed dynamical properties of cumulus convection. Most cumuli exhibit temperatures and liquid water contents much lower than those of undiluted parcels and, due to buoyancy exhaustion, terminate much below the level prescribed by the classical parcel theory. Nevertheless, radar and visual observations of severe thunderstorms have shown tropopause penetrations of a few kilometers on several occasions. Large accelerations are required to produce sufficiently high speeds at the tropopause to accomplish such penetrations. These accelerations cannot be achieved unless the amount of entrainment occurring in the rising updraft is reduced. In the absence of entrain-

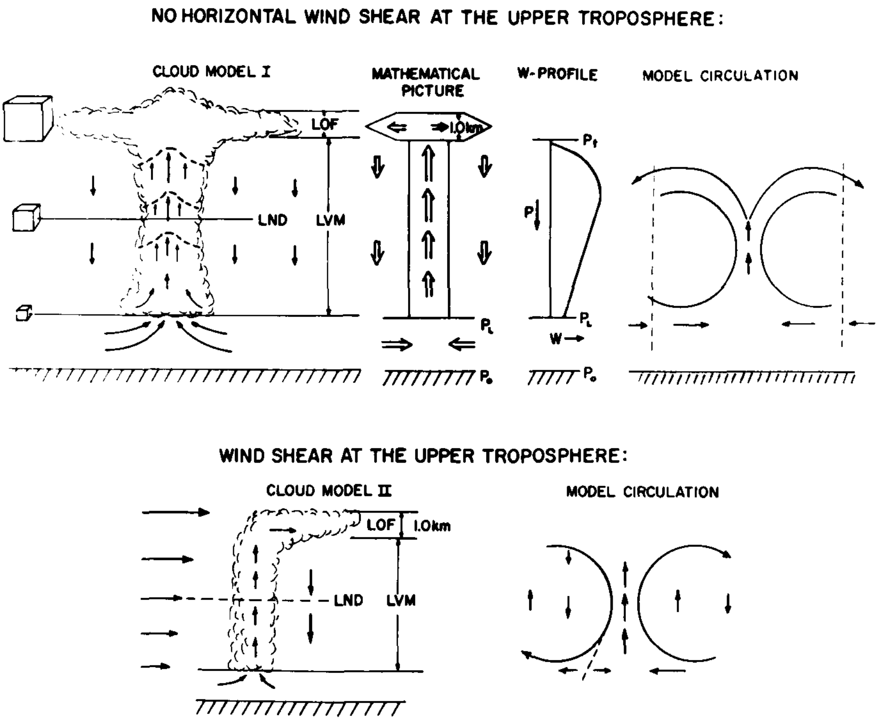

Fig. 1. Schematic diagram for the proposed convection model.

ment, the maximum amount of bouyancy is realized from the condensation process and high velocities are possible. Fujita & Grandoso (1966) have proposed that the entrainment rate is inversely proportional to the cloud diameter. For a giant cloud of 20 km diameter, the entrainment is insignificant under this assumption (Fujita & Grandoso, 1966).

With this hypothesis in mind, a three-layer convection model is proposed for a severe storm. First is the layer of inflow (LOI), extending from the ground to the lifting condensation level (LCL). Second is the layer of vertical motion (LVM), which extends from the LCL to the top of the tower, where the buoyancy is exhausted. The warm moist air drawn in from the LOI is carried upward undiluted in the LVM, rotating cyclonically and losing water as it rises until finally it is ejected out of the storm in the third layer, the layer of outflow (LOF) near the tropopause. The LOF is assumed 1.0 km thick (Ludlum, 1966). The top of this layer is sharply defined by the upper surface of the anvil cloud. On the satellite cloud photographs this glaciated surface appears brighter because of the significantly greater reflectance characteristics of the ice crystals in the visible region of the solar spectrum compared with the reflectance of low and middle clouds composed mainly of water droplets. The cloud brightness, however, depends on many factors, such as cloud form, depth, type, concentration, and the illumination condition.

A schematic diagram of the model is presented in Fig. 1.

2.2 *Computation of latent heat flux*

From the equation of state the volume flux at the LOF is derived as:

$$\frac{dV_0}{dt} = \frac{K}{\varrho_L}\frac{dM_L}{dt} \tag{1}$$

where suffixes 0 and L stand for the base of the LOF and the top of the LOI, respectively; M_L is the mass; ϱ_L is the air density (10^3 g/cm^3) assumed independent of time; and K is a con-

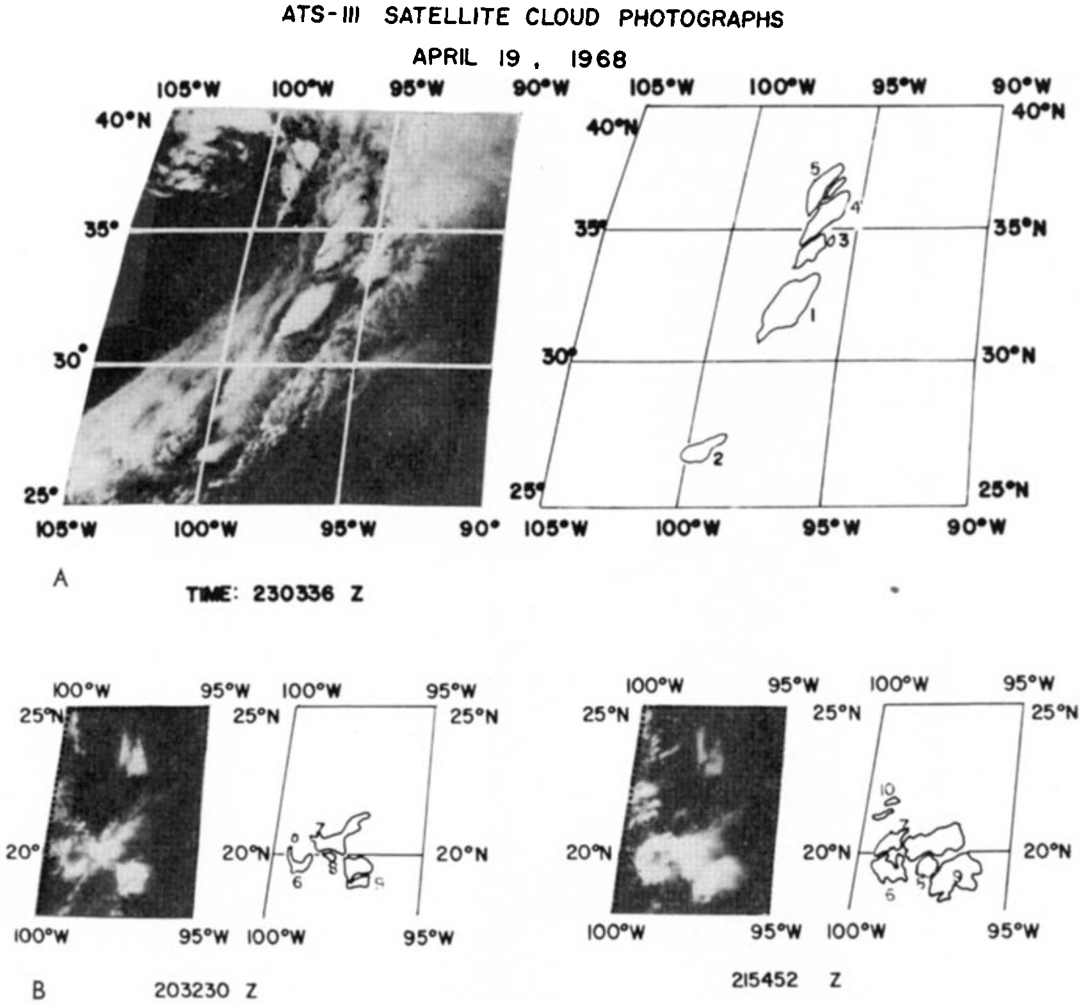

Fig. 2. Severe storm clouds over the United States on April 19, 1968.

stant determined from the environmental upper air soundings.

One can relate the cloud divergence at the LOF to the cloud area change (Sikdar & Suomi, 1968) by:

$$\nabla_H \cdot \mathbf{V}_c = \frac{I}{A_c}\frac{dA_c}{dt} \qquad (2)$$

where suffix c stands for cloud particles and A_c represents the cloud area. This cloud divergence is analogous to the horizontal spread of smoke particles in the atmosphere when a rising smoke plume strikes a stable layer.

From the equations 1 and 2, the mass flux at the cloud base is given by:

$$\frac{dM_L}{dt} = \frac{\varrho_L}{K}\left(\Delta Z \cdot \frac{dA_c}{dt}\right), \text{ g/sec}$$

where $\Delta Z = 1.0$ km (Ludlum, 1966; Borovikov, 1963). The term dA_c/dt is measured from successive ATS pictures.

Assuming that the equivalent potential temperature is constant at the LCL and that all water vapor passes to the condensed phase while ascending through the cloud core, the latent heat flux E_c can be determined from the equation:

$$E_c = L \cdot \Delta W \cdot \frac{dM_L}{dt} \text{ cal/sec}$$

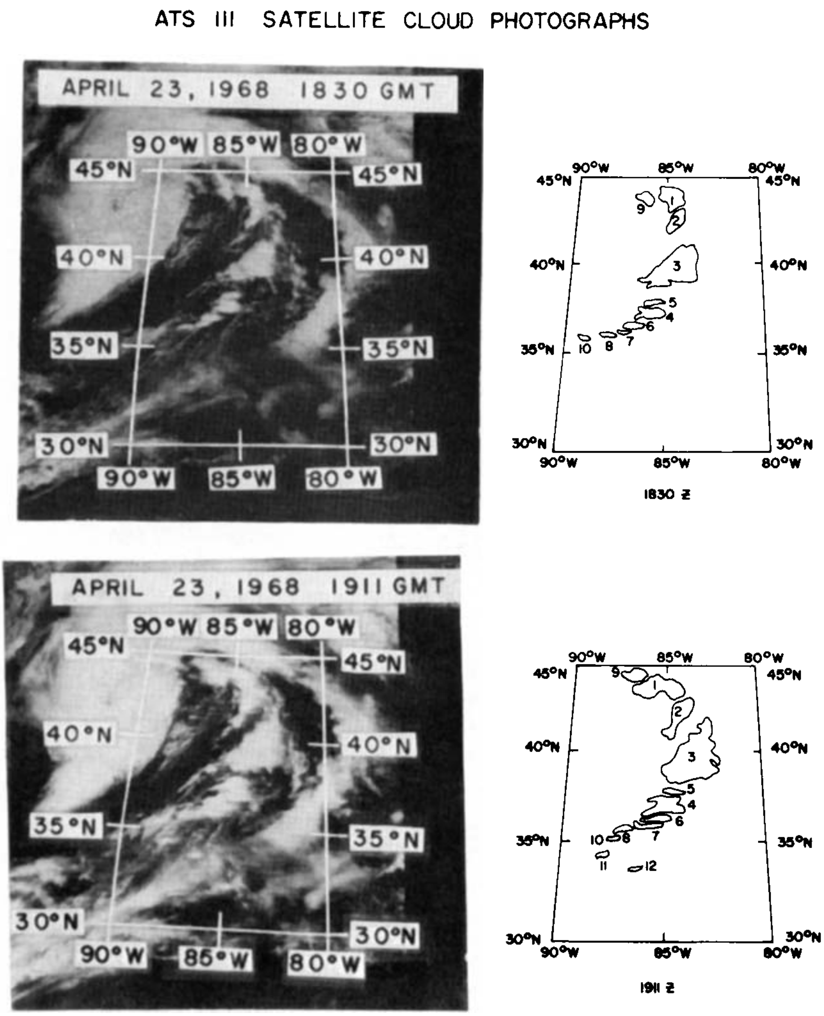

Fig. 3. Severe storm clouds over the United States on April 23, 1968.

where

L = 597 cal/g at 0°C,

$\Delta W = (W_L - W_0)$ g/kg,

W_L = mixing ratio at cloud base,

W_0 = mixing ratio at cloud top.

3. Identification of severe storm on ATS-3 pictures and the technique of their analysis

Cumulus and cumulus congestus largely appear as aggregates on the ATS-111 satellite cloud photographs. Identification of cumulonimbus or storm clouds in the widespread cumulus field is largely a problem of distinguishing their brightness gradients. A uniform field of broken cumulus congestus at best appears as a white haze, whereas a resolved cumulonimbus or a complex of cumulonimbi exhibits strong brightness and well-defined boundaries. Furthermore, on the time-lapse photographs one can easily distinguish the severe storm clouds by their rapid growth rates. On occasions, these rapidly growing storms are associated with clear space in their vicinity. The brightness of these cloud boundaries is significantly enhanced by the presence of a clear zone around them. Figs. 2 and 3 show a few such examples. Cloud samples shown in

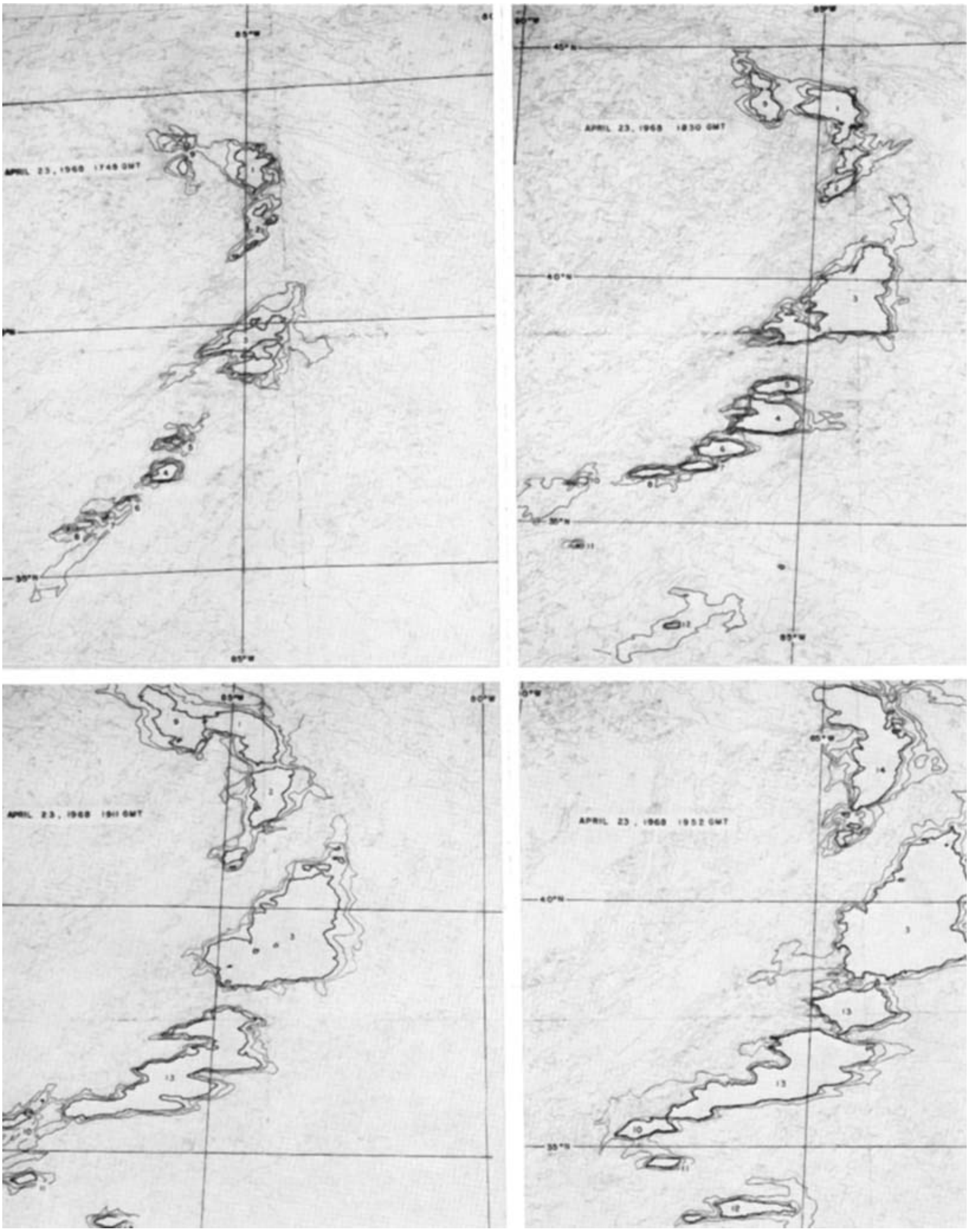

Fig. 4. Brightness contour display of severe storm clouds shown in Fig. 3.

Fig. 2*B* are located over the northern part of Mexico.

The outlines of these identified storm clouds have been tracked on successive satellite photographs, each 14 minutes apart on April 19 and 45 minutes apart on April 23. For a quick estimate of the growth rate of these storm cells this technique seems adequate. For better precision,

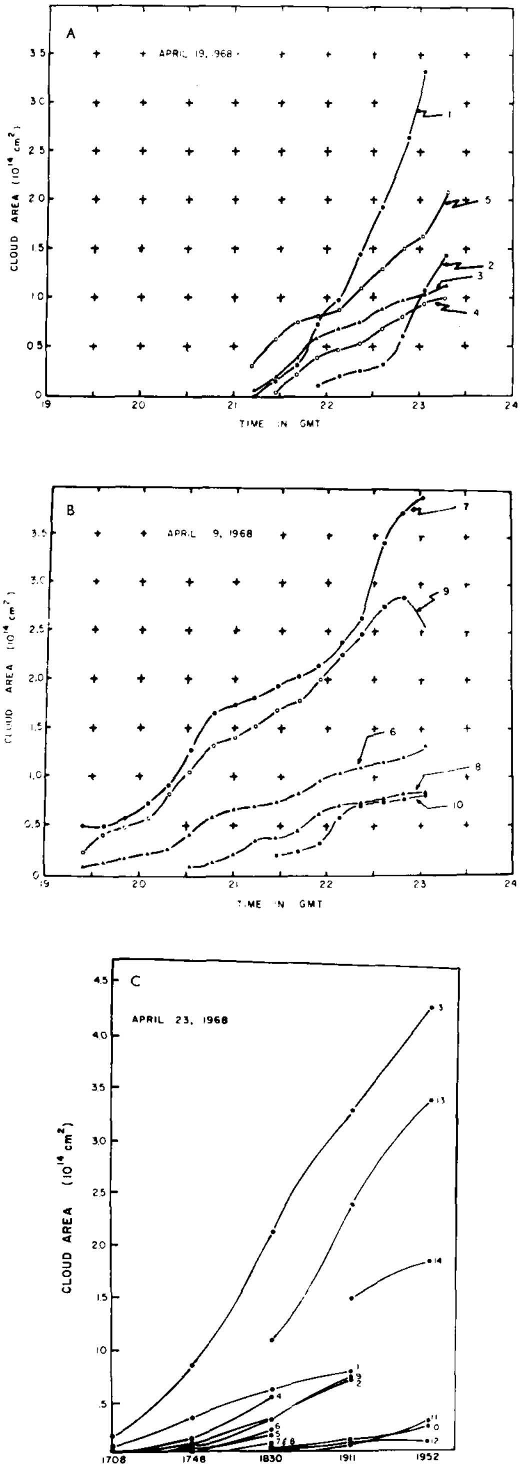

Fig. 5. Cloud area as a function of time.

however, one can measure the area change enclosed by a particular brightness contour corrected for solar zenith angle as a function of time. For example, Fig. 4 shows a photograph of a computer-made brightness contour actually used for preparing the April 23 data set.

Fig. 5 presents the time variation of the area of cirrus canopy evaluated from successive satellite photographs. This diagram clearly indicates a significantly rapid cirrus shield expansion over some of the storm complexes, for example, cloud numbers 1, 2, and 5 on the April 19 and numbers 3 and 13 on the 23rd. These pronounced growth rates obviously reflect on the degree of instability in the concerned region.

The estimates of cloud bases and cloud tops have been made using the parcel technique, from the available afternoon upper air soundings in the vicinity of the storms. Table 1 presents the thermodynamic data used in this computation scheme.

4. Cloud divergences and the severe storm reports over the United States on April 19 and 23, 1968

Fig. 6 presents the cloud divergence as a function of time. These magnitudes represent the averages of a number of storm cells embedded in the complex. In the diagrams of April 19, wide fluctuations in the cloud divergence field can be seen. These fluctuations are probably due to eddies of various sizes participating in severe storm cloud growth. The absence of any such characteristics on April 23 is because of lower sampling frequency.

Fig. 7 presents the plot of severe storm reports over the United States for the 19th and 23rd of April, 1968. The approximate time of occurrence of each severe storm is indicated by a symbol. On April 19, most of the severe storms occurred between 20.00 and 24.00 GMT in Oklahoma and between 00.00 and 06.00 GMT, i.e., in the late evening, in Arkansas and Missouri.

On April 23, widespread severe weather was reported in Michigan, Ohio, Kentucky, and Tennessee in the afternoon hours. The times of occurrence indicate that the severe weather features moved east-northeastward in the late evening. These occurrences of severe weather are clearly related to the cloud systems shown

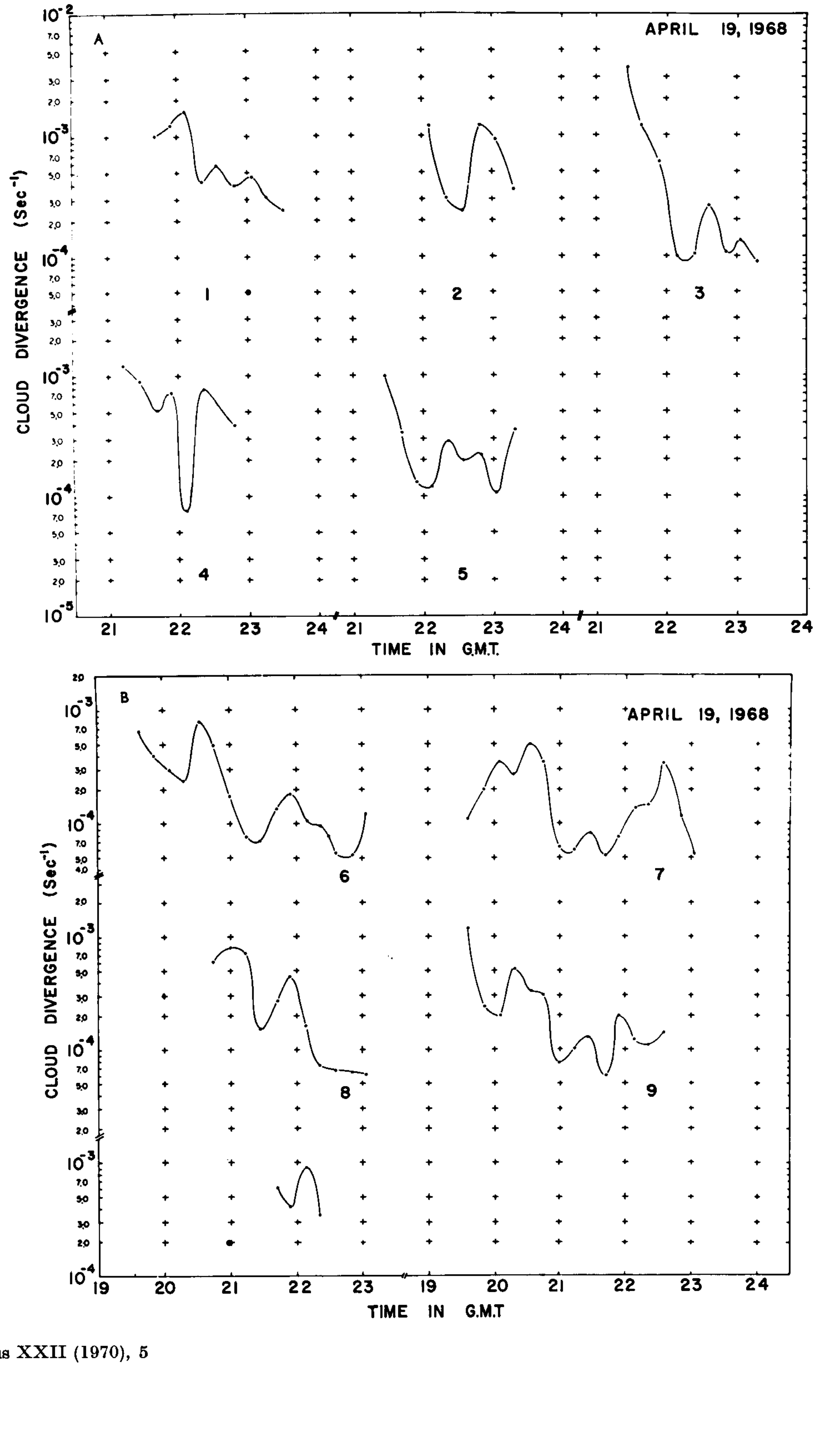
A
APRIL 19, 1968
CLOUD DIVERGENCE (Sec^{-1})
1
2
3
4
5
TIME IN G.M.T.
B
APRIL 19, 1968
CLOUD DIVERGENCE (Sec^{-1})
6
7
8
9
TIME IN G.M.T

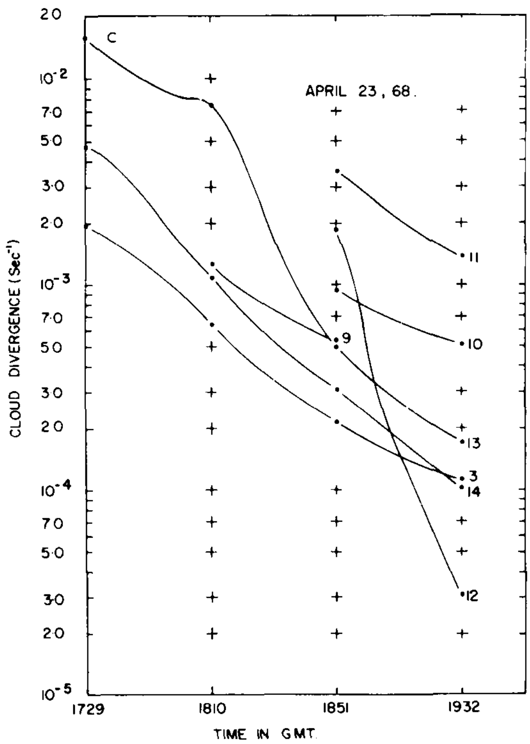

Fig. 6. Cloud divergences in the layer of out flow.

in Fig. 3. The surface reports and satellite data are not adequate to correlate the specific occurrences with the cloud features observed at mesoscale; however, a number of tornados have occurred in cloud complexes 3, 13 and 14 in Fig. 3 on April 23 in the later part of the observation period.

An examination of the times of occurrence of severe weather shown in Fig. 7 and of the corresponding cloud divergence profiles shown in Fig. 6 reveals that most of the severe weather occurred during the partial decay phase of these cloud systems. Furthermore, the cloud divergence profiles on April 23 indicate significantly higher magnitudes in the growth phase than occurred on the 19th. These higher divergence rates are obviously related to the stronger vertical motion field; hence, they might be the reason for greater severity in the storms and higher density of population on April 23. The cloud divergence at the top of an intense convection zone can be calibrated to estimate the probable severity of a particular weather phenomena for the succeeding few hours.

5. Mass and energy fluxes

Fig. 8 presents the time variation of mass influx rate at the subcloud layer for cloud complexes shown in Fig. 2. Fig. 9 shows the model estimates of latent heat fluxes on April 19 and 23.

Brown (1967) has compiled all published data on the convective cloud growth rates (Anderson, 1960; Higuchi, 1965) and has developed a power function to estimate the growth rate and available energy. In an isolated moderate cumulonimbus cloud one expects a mass upward flux of the order of 10^7 kg/sec at lower levels. Braham (1952) also quotes the same order of magnitude for a moderate thunderstorm. Figs. 8 and 9, however, show that the orders of magnitude range from 10^8 to 10_3 kg/sec for the mass upward flux while for the heat flux the range is 10^{12} to 10^{13} cal/sec, about one to two orders of magnitude higher than in an ordinary thunderstorm.

Fig. 9 *B* refers to the upward energy fluxes associated with a number of severe storms

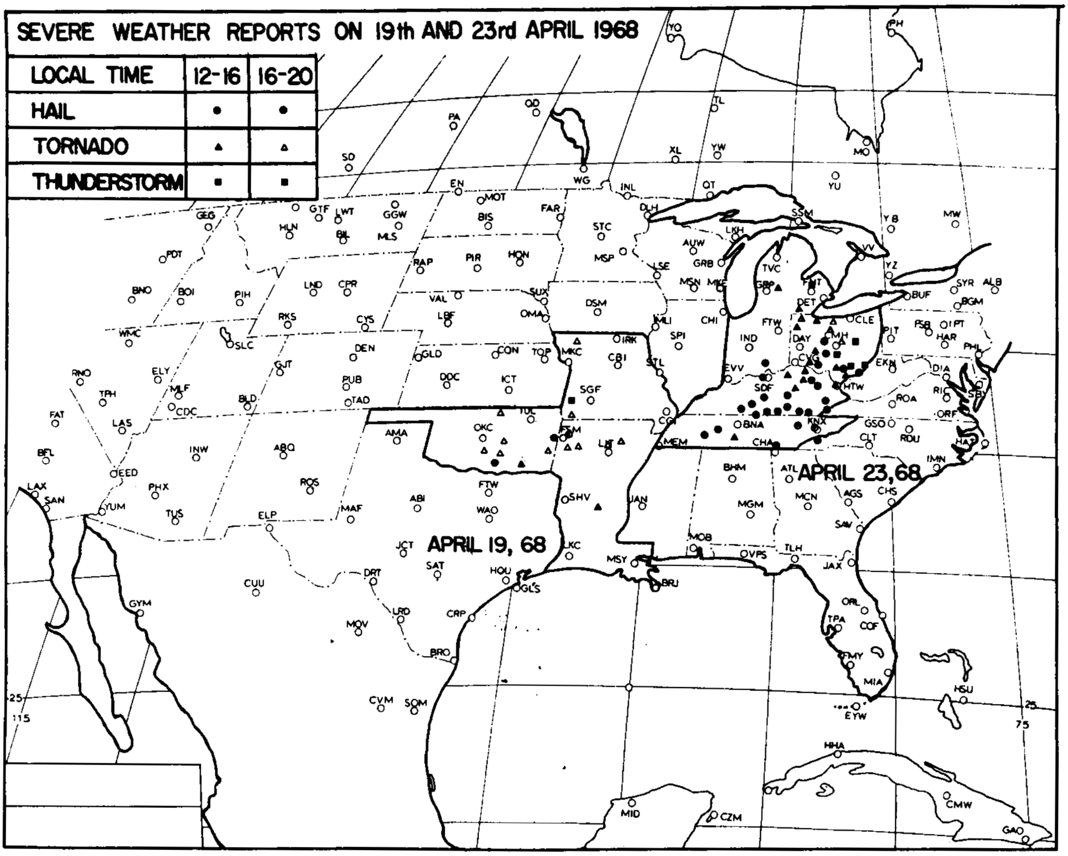

Fig. 7. Regions of severe weather over the United States on 19th and 23rd of April, 1968.

(see Fig. 2*B*) occurring over Mexico (around 20° N) on April 19. These clouds show a strong fluctuation in the vertical transport of heat and mass. Here again, the magnitudes of energy fluxes are greater by at least one order of magnitude compared with that of a moderate thunderstorm, although their cloud structures are appreciably different from those shown in Figs. 2*A* and 3. These clouds exhibit structures with ill-defined fuzzy edges. The absence of sharp boundaries in these cloud systems may be attributed to the lesser moisture contrast between the cloud periphery and the clear zones, a feature generally observed in the subtropical convective systems. No definite reason for this structural difference is known to us at present. It is possible that in the subtropical storm clouds the subsidence is important at low levels.

Table 1. *Thermodynamic data*

	Cloud (mb)		Mixing ratio (g/kg)		Temperature (°K)	
Date	Base	Top	W_L	W_0	T_L	T_0
April 19, 1968	930	220	10	0.1	298	215
April 23, 1968	780	330	6	0.3	278	233

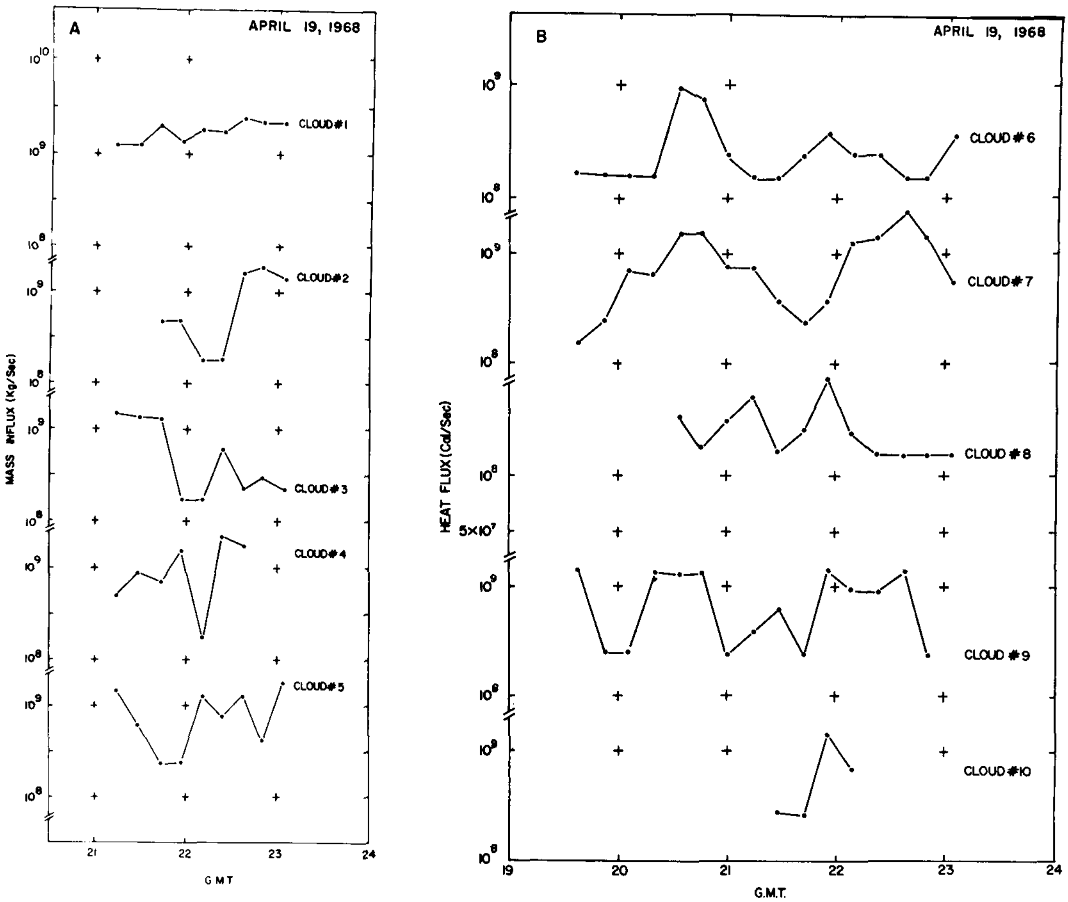

Fig. 8. Mass influx at the sub-cloud layer as a function of time.

6. Summary

In this paper we have shown that the convective systems causing severe weather along the frontal zones in the mid-latitude disturbance field can be identified and tracked on the ATS-3 satellite time-lapse photographs. The severity of weather can probably be assessed from the growth rate of these cloud systems. A convective cloud complex indicating an average cloud divergence (6.0×10^{-4} sec^{-1} or more) in the layer of cirrus outflow is likely to be associated with severe weather, such as heavy thundershower, hail, and tornados. Most of these active convective systems transport latent heat to the upper troposphere in magnitude at least one order higher than in a moderate thunderstorm.

Another interesting feature observed is the occurrence of severe weather in these identified clouds during the period when these cloud systems enter into a partial decay phase. This is clearly shown in the cloud divergence profile as a function of time.

7. Future research

The magnitude of cloud divergence at the layer of cirrus outflow is also an indication of the character of vertical motion field in the embedded "hot towers". With the upward mass flux measurements available with the technique, one can estimate the average vertical motion field, provided the areas of the updraft core are known from the radar echoes or by some other technique such as image enhancement of the brightest portions of the photo.

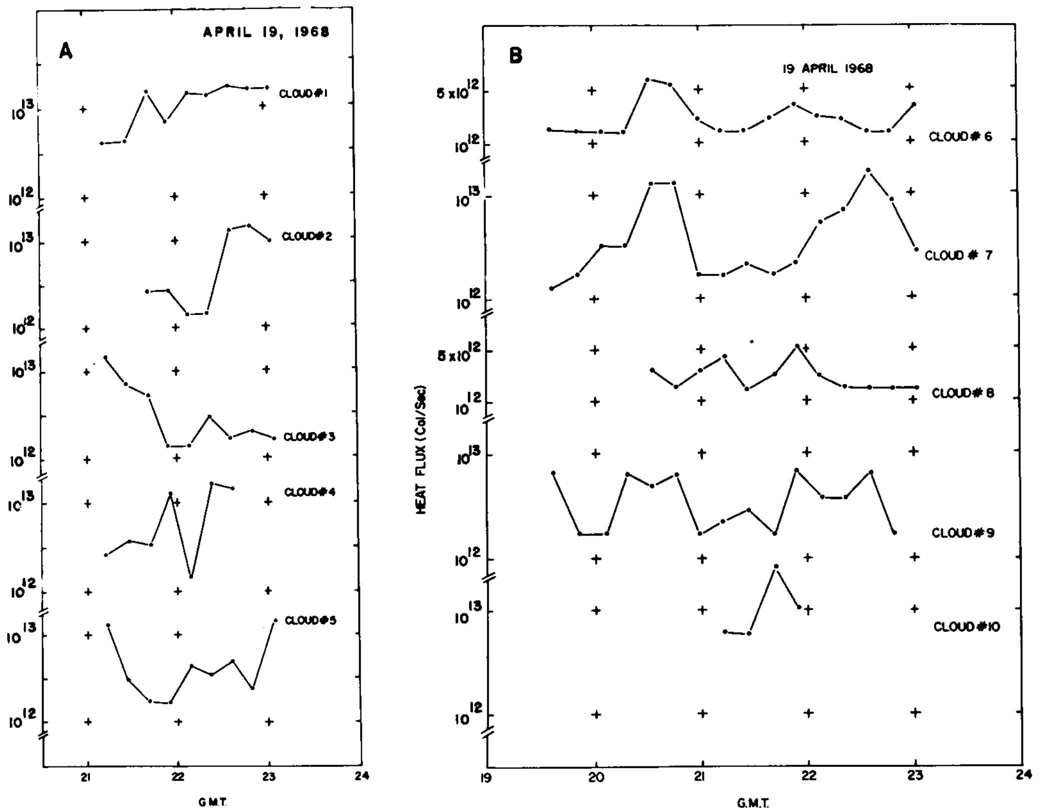

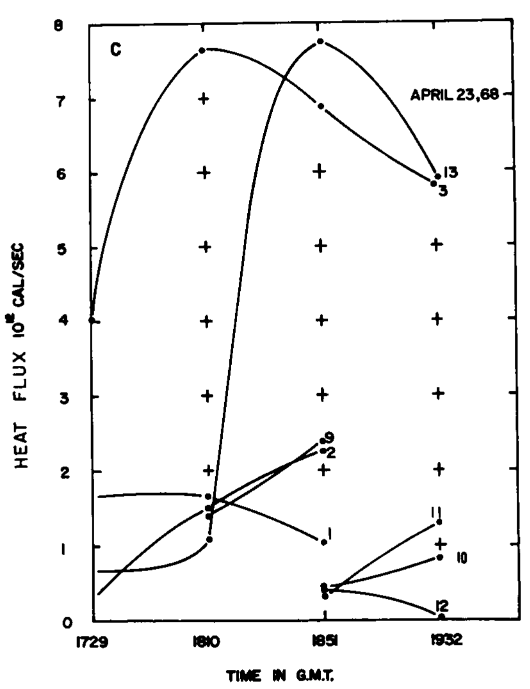

An objective method of estimating the average vertical motion field in severe storms from the ATS-3 photographs is being developed and will be communicated shortly. Since the vertical motion field in a storm system has a unique correlation with the rainfall rate, it may be possible to estimate the average amount of precipitation associated with this kind of growing cloud system.

8. Acknowledgement

The authors wish to thank Mr. Brian Auvine for measuring the cloud areas and procuring thermodynamic data for the April 23 case presented in this paper. Thanks are also due to Mr. Eric Smith, who programmed for the brightness contour display. This investigation was supported in part by the US Weather Bureau under Grant WBG 27 and partly by NASA under Grant 11542.

Fig. 9. Convective heat fluxes in severe storms as a function of time.

REFERENCES

Anderson, C. E. 1960. A study of the pulsating growth of cumulus clouds. *Geophysical research paper no. 72*. Air Force Cambridges Res. Lab., Mass., 136 pp.

Borovikov, A. M. et al. 1963. *Cloud physics*. U.S. Dept. of Commerce, Washington, D.C.

Braham, R. R. 1952. The water and energy budgets of the thunderstorm and their relation to thunderstorm development, *J. Meteor.*, 227–242.

Brown, R. A. 1967. Mass and available energy in growing convective cloud, *J. Atm. Sci. 24*, 308–311.

Fujita, T. & Grandoso, H. 1966. Split of a thunderstorm into anticyclonic and cyclonic storms and their motion as determined from numerical model experiments. *SMRP research paper no. 62*, University of Chicago.

Higuchi, K. 1965. A three-dimensional study of cumulus cloud by the use of aerial photographs of the clouds and their shadows. *J. Atmos. Sci. 22*, 440–447.

Ludlum, F. H. 1966. Cumulus and cumulonimbus convection, *Tellus 8*, 4, 687.

Sikdar, D. N. 1969. Convective heat transport over the tropical mid-Pacific as estimated from a geosynchronous satellite altitude. Ph.D. thesis, The University of Wisconsin, Madison, Wisc.

Sikdar, D. N. & Suomi, V. E. 1968. An objective technique of evaluating tropical mesoscale heat transport in the tropics from geosynchronous satellite photographs. *Studies in atmospheric energetics based on aerospace probings*. 1968 Annual Report, Department of Meteorology, The University of Wisconsin, Madison, Wisc.

The Thunderstorm, 1959. US Government Printing Office, Washington, D.C.

US Department of Commerce, 1968. *Storm Data*, vol. *10*, 4.

КОНВЕКТИВНЫЙ ПЕРЕНОС МАССЫ И ЭНЕРГИИ В СИЛЬНЫХ УРАГАНАХ НАД СОЕДИНЕННЫМИ ШТАТАМИ — ОЦЕНКА С ГЕОСТАЦИОНАРНОГО СПУТНИКА

Некоторые важные характеристики интенсивности конвекции, связанной с вихрями ураганов, описываются на основе фотографий территории США, снятых 19 и 23 апреля 1968 г. на геосинхронном спутнике NASA ATS-III. Изучаются скорости роста ряда конвективных комплексов, имеющихся на фотографиях облачного покрова. На основе трехслойной модели конвекции вычисляются вертикальные потоки массы и энергии в этих сильных ураганах. Вычисленные потоки представляются бóльшими по крайней мере на порядок величины, чем в умеренных грозах (Brown, 1967). Предположено, что ярко выраженная скорость роста конвективного комплекса, оцененная с помощью фотографий ATS-III, должна указывать на присутствие ячеек сильных ураганов под покровом перистых облаков.